Analytic Solutions for Pulse Propagation in Shielded Power Cable for Symmetric and Asymmetric PD Pulses

Naima Oussalah, **Youcef Zebboudj**
Laboratoire de Genie Electrique
University A.Mira. of Bejaia
Bejaia, Algeria

and **Steven A. Boggs**
Institute of Materials Science
Departments of Electrical Engineering & Physics
University of Connecticut
Storrs, CT 06269-3136
Department of Electrical and Computer Engineering
University of Toronto

ABSTRACT

Shielded power cable can be considered as a lossy transmission line, the high frequency attenuation of which causes the PD pulse amplitude, as well as the pulse energy, to decrease as a function of distance propagated. We develop analytical expressions which characterize PD pulse propagation in a shielded power cable for both symmetric and asymmetric PD pulse waveforms for an attenuation constant which increases linearly with frequency.

Index Terms — **Partial discharge, shield power cable, high frequency propagation.**

1 INTRODUCTION

A 1982 paper [1] defined the fundamental limits to electrical detection of corona and partial discharge, i.e., wideband detection of a partial discharge (PD)-induced pulse in the presence of thermal or Johnson noise, including the effect of frequency-dependent attenuation in shielded power cable. Most of the plots in [1] were the result of numerical computations. Software tools now facilitate an analytic solution for all parameters of interest. The purpose of this paper is to provide the most rigorous possible analytical solutions to PD pulse propagation in shielded power cable for both symmetric (Gaussian) and asymmetric PD pulse waveforms in the approximation that the attenuation constant (dB/m or Nepers/m) of the cable is proportional to frequency, as is normally true for shielded power cable for frequencies above 1 MHz. Based on our objective, we must ignore such effects as dispersion and frequency dependent characteristic impedance, the inclusion of which would preclude an analytic solution. A preliminary version of the present analysis was published in [2]. The present version cleans up a number of technical issues and presents computed data in a more usable form. It also includes a discussion of the implications of the analysis for PD detection sensitivity in shielded power cable.

Manuscript received on 9 August 2006, in final form 20 May 2007.

2 HIGH FREQUENCY ATTENUATION

For XLPE cable, which is the main subject of PD measurements in distribution systems, high frequency attenuation is caused mainly by the shield layers [3]. While the properties of cable shields can vary widely, they typically have conductivity in the range of 0.1 to 1 S/m and a relative dielectric constant in the MHz range of a few hundred. Figure 1 shows measured attenuation data for two, 15 kV class concentric neutral XLPE cables, one a 22 year old XLPE cable removed from service and the other a recently manufactured TR-XLPE cable. The measured attenuation for the 22 year old XLPE cable is very noisy as a result of its short length; however, the frequency dependent attenuation of the two cables is clearly very similar. From a wide range of past measurements, the attenuation of these two cables, which can be written as $\alpha\omega L$ Nepers, where α is a constant, ω is radial frequency, and L is cable length, $\alpha=5\text{x}10^{-11}$ Nepers/s-m is typical and will be used for most examples in the present analysis. Since analytic equations will be provided for all parameters of interest, other attenuations could be substituted, as appropriate.

As in the introduction, dispersion, the variation of propagation velocity with frequency, is appreciable in shielded power cable but is not included in the present analysis, as the objective of the present analysis is to provide the most complete available analytic solutions for the parameters of interest, and analytic solutions which include the effects of dispersion are unlikely. The frequency dependence of the characteristic impedance is ignored for the same reasons.

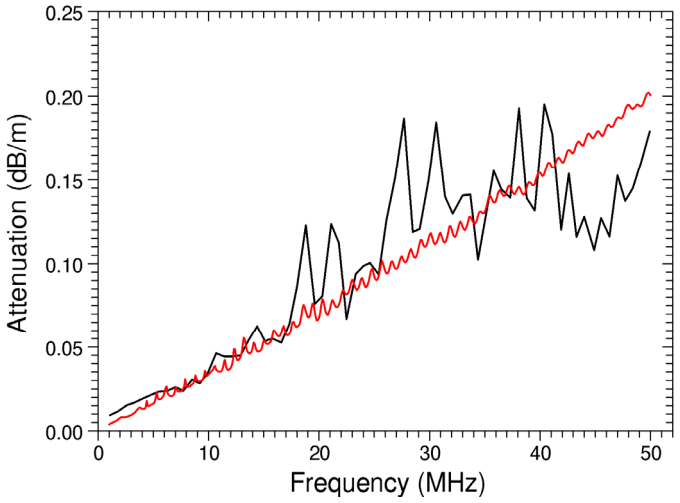

Figure 1. Measured attenuation for two 15 kV class concentric neutral XLPE cables. The black, noisy line provides the measured attenuation of a 22 year old XLPE cable while the red, smooth line provides the attenuation of a recent TR-XLPE cable. The measurement of the older cable is noisy as the sample was rather short.

3 PD PULSE PROPAGATION

3.1 GAUSSIAN PULSE

We start by assuming that the PD pulse is generated by a Gaussian current propagating in the conductor, i.e.

$$I(t) = I_o \exp\left(-\frac{t^2}{2\sigma^2}\right) \tag{1}$$

where I_0 is the peak pulse current amplitude and the pulse width (full width at half maximum or FWHM) is 2.36 σ. The partial discharge magnitude of this pulse is given by

$$Q = \int I(t)\,dt = I_0\,\sigma\sqrt{2\pi} = \frac{V_0\,\sigma\sqrt{2\pi}}{Z} \tag{2}$$

where $V_0 = I_0 Z = I_0 Zc/2$ is the peak voltage and Zc is the cable characteristic impedance. Thus the voltage waveform is

$$V(t) = V_0 \exp\left(-\frac{t^2}{2\sigma^2}\right) = \frac{Q\,Zc}{2\sigma\sqrt{2\pi}} \exp\left(-\frac{t^2}{2\sigma^2}\right) \tag{3}$$

where Q is the partial discharge magnitude (C).

As is well known, the Fourier transform of a Gaussian is a Gaussian,

$$V(\omega) = Q\,Z \exp\left(-\frac{1}{2}\omega^2\,\sigma^2\right) \tag{4}$$

We now multiply by the frequency dependent attenuation,

$$V_A(\omega) = Q\,Z \exp\left(-\frac{1}{2}\omega^2\,\sigma^2\right) \exp\left(-\omega\alpha L\right) \tag{5}$$

and transform this back into the time domain, obtaining,

$$V_A(t) = \frac{Q\,Zc}{4\sigma\sqrt{2\pi}}\left[\exp\left(A^2\right)\operatorname{erfc}\left(A\right) + \exp\left(B^2\right)\operatorname{erfc}\left(B\right)\right] \tag{6}$$

where erfc is the complementary error function (1-erf) and

$$A = \left(\frac{\alpha L + jt}{\sqrt{2}\,\sigma}\right),\; B = \left(\frac{\alpha L - jt}{\sqrt{2}\,\sigma}\right) \tag{7}$$

where α is the attenuation factor, L is the distance propagated by the PD pulse, t is time, σ characterizes the initial pulse width as described above, and $j = \sqrt{-1}$.

Equation 6 gives the pulse waveform as a function of distance propagated, attenuation constant, and initial pulse width (2.36 σ FWHM). This equation can be difficult to evaluate, as for typical conditions, $\exp(A^2)$ becomes very large at large distances, while erfc(A) becomes extremely small. However the equation has been evaluated successfully using Maple.

The peak pulse amplitude can be obtained by setting t=0,

$$V_p(L) = \frac{QZc}{2\sigma\sqrt{2\pi}}\left(\exp\left(\frac{\alpha^2 L^2}{2\sigma^2}\right)\operatorname{erfc}\left(\frac{\alpha L}{\sigma\sqrt{2}}\right)\right) \tag{8}$$

As the pulse propagates down the cable, it loses high frequency energy, resulting in a reduction in the optimum bandwidth for detection which can be taken as roughly the -6 dB bandwidth [1]. From eqn. (5), we can determine the -6 dB bandwidth (Hz) as

$$BW(L) = \frac{-\alpha L + \sqrt{\alpha^2 L^2 + 2\sigma^2 \ln(2)}}{2\pi\sigma^2} \tag{9}$$

so that the -6 dB bandwidth for the 1.2 ns FWHM Gaussian pulse at inception is about 370 MHz, and this decreases to about 20 MHz after propagating roughly 100 m down the cable, which explains why typical detection bandwidths are in the range of 10 to 20 MHz.

As noted above, the Fourier transform of a Gaussian is a Gaussian. In eqn. (4), this Gaussian in the frequency domain is weighted by the frequency-dependent attenuation in order to compute the attenuated waveform in the time domain. After weighting in the frequency domain, the spectral distribution is no longer Gaussian, which means that in the time domain, the pulse waveform is no longer Gaussian. The waveform after attenuation, eqn. (6), is a complicated function, and we have not been able to obtain an analytical solution for the pulse width (FWHM) as a function of distance, although a numerical solution is possible, as shown in Figure 2. The pulse width can be approximated by assuming that the pulse after frequency dependent attenuation is Gaussian. In this approximation, the pulse width as a function of distance

propagated is given by

$$PW(L) = \frac{2.36\sigma}{\exp\left(\frac{\alpha^2 L^2}{2\sigma^2}\right)\operatorname{erfc}\left(\frac{\alpha L}{\sigma\sqrt{2}}\right)} \tag{10}$$

and the energy in the pulse is given by

$$W(L) = \frac{Q^2 Zc}{4\sigma\sqrt{\pi}}\left[\exp\left(\frac{\alpha^2 L^2}{2\sigma^2}\right)\operatorname{erfc}\left(\frac{\alpha L}{\sigma\sqrt{2}}\right)\right] \tag{11}$$

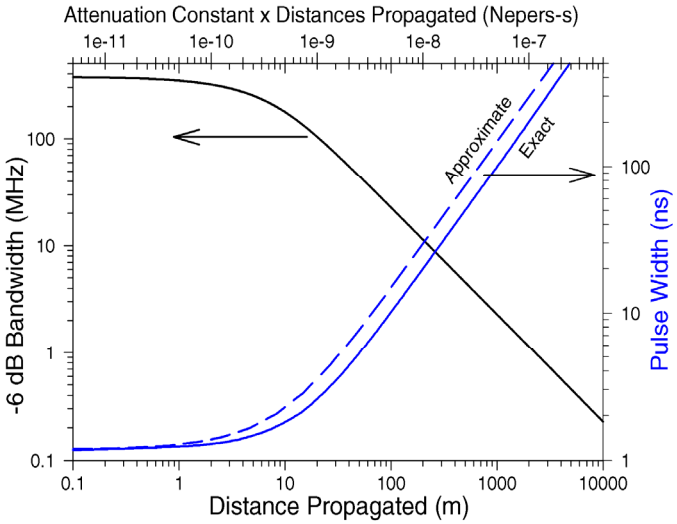

Figure 2. Pulse -6 dB bandwidth as a function of distance propagated. At 0 distance, the bandwidth is about 370 MHz for an attenuation constant of $5\text{x}10^{-11}$ s/m. However at 1000 m, the bandwidth is in the range of 1 MHz, well below the typical detection bandwidth of field PD measurement systems of about 10 MHz. The exact pulse width, as determined numerically, is shown along with an analytic approximation for the pulse width.

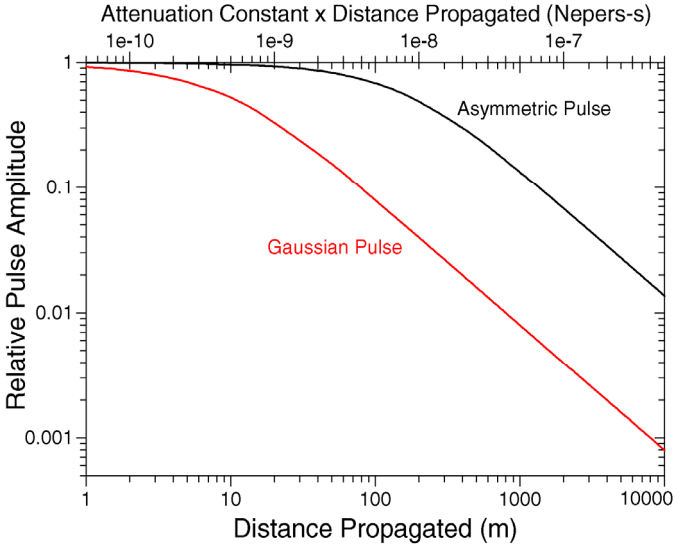

Figure 3. Relative peak voltage as a function distance propagated for a Gaussian pulse with a pulse width (FWHM) of 1.2 ns and for an asymmetric pulse and attenuation constant of $5\text{x}10^{-11}$ Nepers-s/m.

3.2 ASYMMETRIC PULSE

We model the measured PD waveform of Figure 4 as a sum of Gaussians, a plot of which is also shown in Figure 4,

$$I(t) = I_0\sum_{i=1}^{60}\left(A_0(i)\exp\left(-\frac{\left(t-t_0(i)\right)^2}{2\sigma_0(i)^2}\right)\right) \text{ where} \tag{12}$$

$$A_0(i) = \frac{0.2245}{\sqrt{\exp\left(\frac{i}{5}\right)}},\ \sigma_0(i) = 10^{-9}\frac{\exp\left(i^{0.25}\right)}{\sqrt{2}},\ t_0(i) = \frac{i+5000}{10^9}$$

which results in a peak current of I_0 and charge of $2.15\text{x}10^{-8}$ I_0.

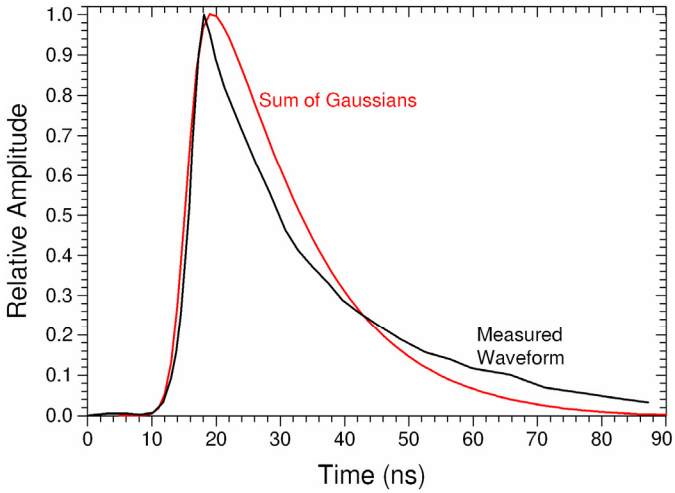

Figure 4. Measured asymmetric PD waveform provided by Prof. Lemke along with the sum of Gaussians used to simulate the measured waveform [4].

The pulse charge (time integral of current) can be written as

$$Q = \int I(t)\,dt = \sum_{i=1}^{60} I_0 A_0(i)\sigma_0(i)\sqrt{2\pi}\,, \text{ or} \tag{13}$$

$$Q = \sum_{i=1}^{60}\frac{V_0 A_0(i)\sigma_0(i)\sqrt{2\pi}}{Z} \tag{14}$$

where $V_0 = I_0 Z = I_0 Zc/2$. Thus the voltage waveform is

$$V(t) = V_0\sum_{i=1}^{60}\left(A_0(i)\exp\left(-\frac{\left(t-t_0(i)\right)^2}{2\sigma_0(i)^2}\right)\right) \tag{15}$$

We can compute the waveform as a function of distance propagated by noting that for each Gaussian in the sum, we can take a Fourier transform, multiply by the cable attenuation, and transform back into the time domain, as was implemented for a single Gaussian PD pulse above (eqn. (6)). Thus the waveform after propagating a distance L is just the sum of the resulting waveforms after this process. As noted above, eqn. (6) and hence eqns. (16-18) are difficult to evaluate as they involve sums of products of very large numbers times very small numbers. We can develop an approximate solution by assuming that the attenuated Gaussian components remain Gaussian with a distance-dependent standard deviation of eqn. (16) and amplitude of eqn. (17), which results in an approximate waveform given by eqn. (18).

$$\sigma_i(L) = \frac{\sigma_0(i)}{\exp\left(\frac{\alpha^2 L^2}{2\sigma_0(i)^2}\right)\operatorname{erfc}\left(\frac{\alpha L}{\sigma_0(i)\sqrt{2}}\right)} \tag{16}$$

$$A_i(L) = A_0(i)\left(\exp\left(\frac{\alpha^2 L^2}{2\sigma_0(i)^2}\right)\operatorname{erfc}\left(\frac{\alpha L}{\sigma_0(i)\sqrt{2}}\right)\right) \tag{17}$$

$$V(t,L) = V_0\sum_{i=1}^{60}\left(A_i(L)\exp\left(-\frac{(t-t_0(i))^2}{2\sigma_i(L)^2}\right)\right). \tag{18}$$

Figure 5 shows the pulse amplitude as a function of distance propagated for the asymmetric pulse based on the exact solution and the approximation of eqn. (18). Figure 6 shows a comparison of the exact and approximate waveforms as a function of distance. The approximate solution of eqn. (18) appears to be accurate to within 10% over the full range of distance, which is adequate for the purposes of PD detection.

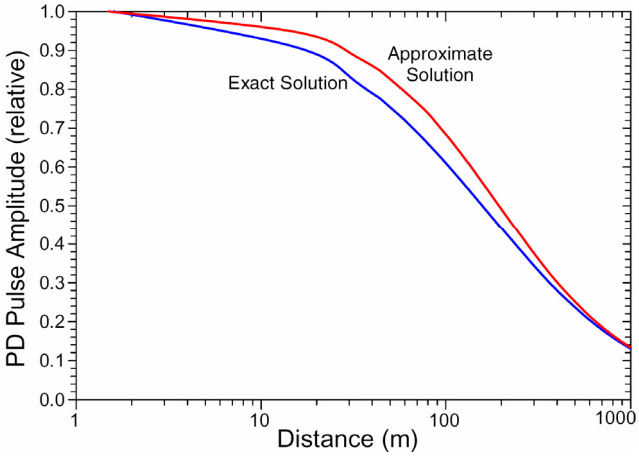

Figure 5. Asymmetric PD pulse amplitude as a function of distance propagated for the exact and approximate solutions with an attenuation constant of $5\text{x}10^{-11}$ s/m. The approximate solution appears to be accurate to within 10% over the full range of distance.

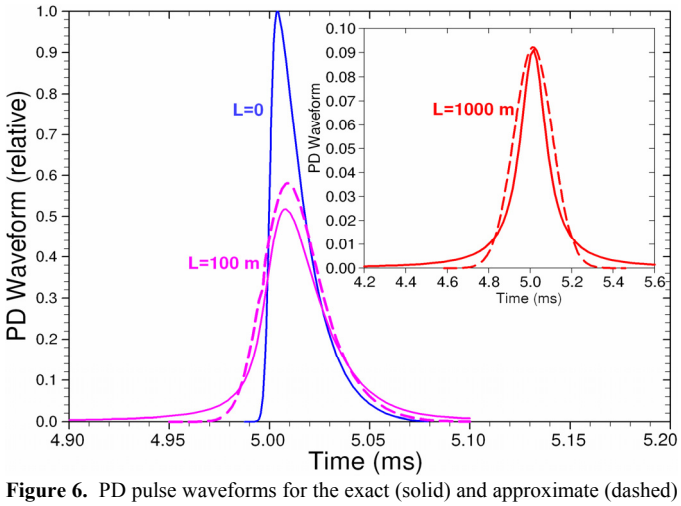

Figure 6. PD pulse waveforms for the exact (solid) and approximate (dashed) solutions.

This process can be applied to any waveform which can be written as a sum of Gaussians, and essentially any waveform can be written as a sum of Gaussians, from triangular to rectangular pulses. Thus this approach provides a very general formulation for propagation of an essentially arbitrary pulse on a shielded cable subject to the assumptions given above, the most important of which is the form of the frequency dependent attenuation.

The PD pulse amplitude for a 1 pC pulse as a function of distance propagated is shown in Figure 7. As would be expected of a broader waveform with longer risetime, the asymmetric PD pulse attenuates less rapidly at small distances than the much narrower Gaussian PD pulse. Figure 8 shows the -3 dB bandwidths for the Gaussian and asymmetric pulses. Both the peak amplitude and -3 dB bandwidth for the Gaussian and asymmetric pulses converge for propagation distances greater than a few hundred metres, as the pulse shape and bandwidth are dominated by the high frequency attenuation.

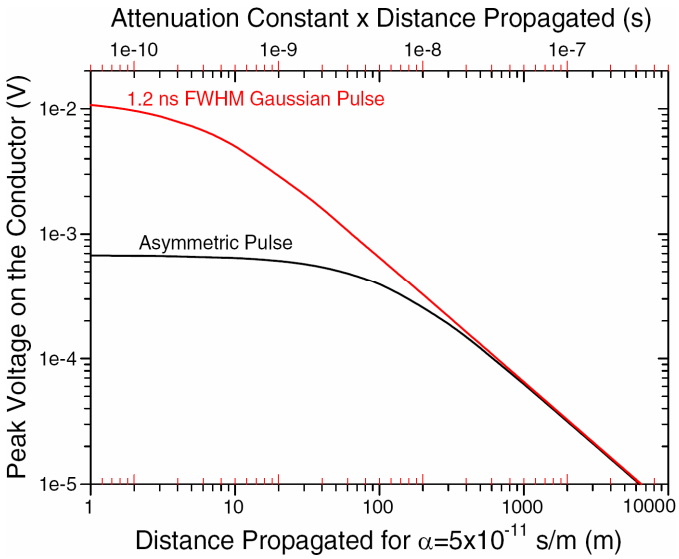

Figure 7. Peak voltage on the conductor for a 1 pC 1.2 ns (FWHM) Gaussian PD pulse and a 1 pC asymmetric PD pulse propagating on a cable with a 30 Ω characteristic impedance. Beyond a few hundred metres, the pulse amplitudes merge, as the total charge in each pulse is the same, and the effective bandwidth is small compared to the initial bandwidth of either pulse.

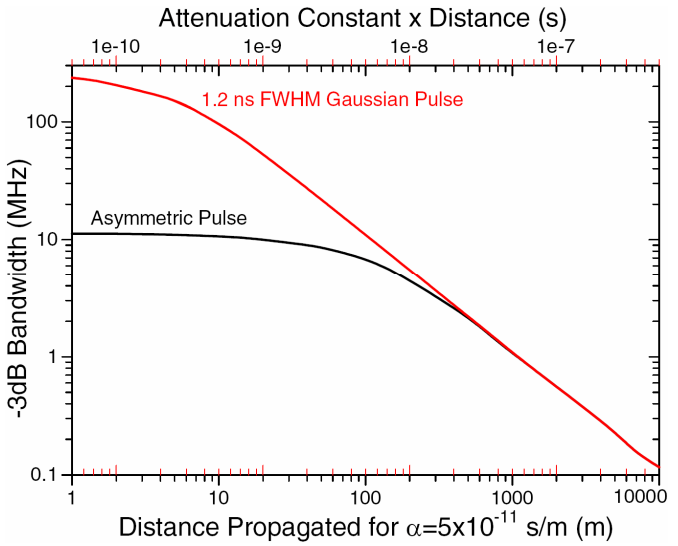

Figure 8. -3 dB bandwidth as a function of distance propagated for a 1.2 ns (FWHM) Gaussian PD pulse and an asymmetric PD pulse propagating on a cable with a 30 Ω characteristic impedance and an attenuation constant of $5\text{x}10^{-11}$ s/m. Beyond a few hundred metres, the bandwidths merge.

4 IMPLICATIONS FOR PD DETECTION

4.1 NOISE ON THE CABLE

The spectral distribution of noise on the cable during measurement of partial discharge varies depending on the local environment. However we can obtain an idea of the typical noise by averaging over a number of locations. Figure 9 shows such data corrected for the PD coupler response and for the gain in the measurement electronics. These data were measured with a 1 MHz bandwidth. An examination of the data in the range up to 50 MHz suggests a noise floor in the range of 3 mV, which implies a noise voltage density of about 3 μV/√Hz.

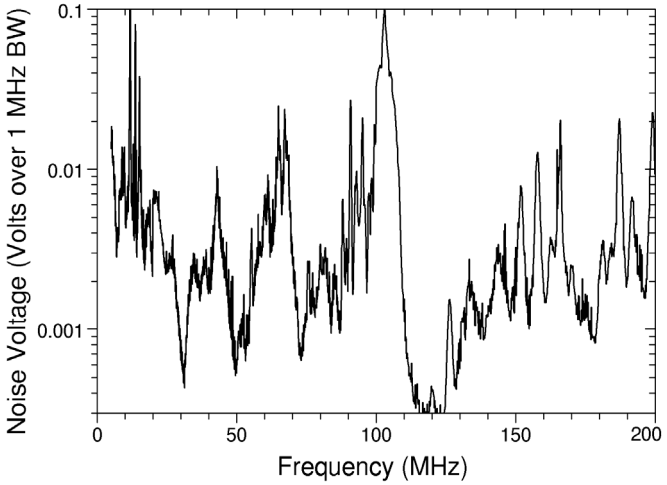

Figure 9. Measured average noise spectrum on cables in urban/industrial environments after correction for PD coupler response and for gain in the measurement electronics. Over the frequency range up to 50 MHz, an average noise floor of about 3 mV seems reasonable. Given a 1 MHz measurement bandwidth, this corresponds to 3 μV/√Hz .

4.2 MATCHED FILTER

As discussed in detail in [5], a matched filter is very difficult to implement for detection of partial discharge propagating on a cable, as the waveform changes, which means that a bank of filters is required, each near optimum for a range of distances propagated. In the case of a Gaussian PD signal propagating in white noise, a rectangular filter of optimum bandwidth comes very close (within about 1 dB) of a matched filter [1]. Thus in this case, the change in the -6 dB bandwidth of the pulse gives an indication of the optimum detection bandwidth. Figure 10 shows the near-optimum detection bandwidth as a function of distance propagated for a pulse which starts out with at 1.2 ns FWHM (σ = 0.5 ns) and for the asymmetric pulse of Figure 4.

The signal to noise ratio for a Gaussian pulse detected in white noise is simply W/S, where W is the energy in the pulse, and S is the spectral noise power density (W/Hz). Based on the above value for the average noise voltage of 3 μV/√Hz, $S=7.5\times10^{-14}$ W/Hz. We can compute the PD detection sensitivity based on a 10 dB signal to noise ratio as a function of distance propagated by using equation (11) for the energy in the pulse and the above value for S. This results in a detection sensitivity for 10 dB S/N ratio shown by the line labeled "Matched Filter" in Figure 10. For a matched filter, the effecttive detection bandwidth varies with distance, as at large distances, no useful signal remains. The line which corresponds to the right axis gives the near-optimum (-6 dB) bandwidth as a function of distance. Note that this bandwidth varies from about 370 MHz at very short distances to about 0.5 MHz at 3000 m.

4.3 DETECTION OF A VOLTAGE PULSE IN NOISE

If we used voltage detection by triggering above the noise, the sensitivity is reduced, as the peak noise is about 4 times the RMS voltage. For voltage detection with optimum bandwidth (Figure 10), the sensitivity is about a factor of 4 worse than for the matched filter with the same 10 dB S/N.

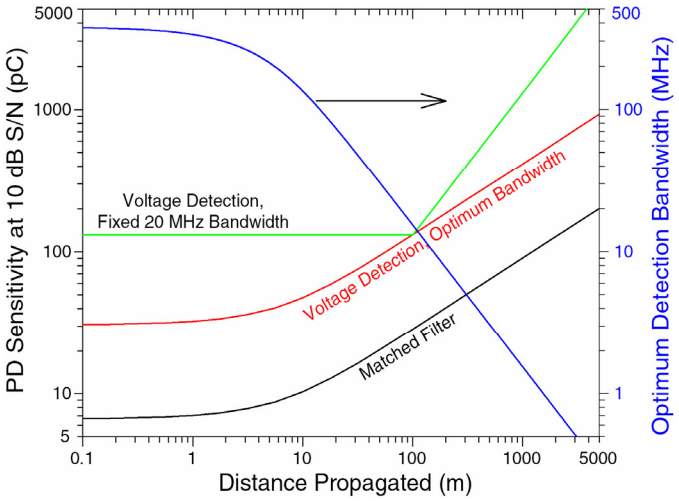

Figure 10. PD detection sensitivity for a 1.2 ns FWHM Gaussian PD pulse and 10 dB signal to noise ratio as a function of distance propagated by the PD pulse based on the parameters given in the text. The bandwidth is based on - 6 dB [1].

If we fix the bandwidth at 20 MHz, which is more typical of engineering solutions to field PD detection, then we obtain the PD detection sensitivity for voltage detection with the peak PD signal 10 dB (a factor of 3.16) above the "peak" noise also shown in Figure 10. In this case, the detection sensitivity suffers at short distances, as not all the useful signal energy is being detected, and the sensitivity suffers at large distances because the bandwidth is greater than optimum, which means that high frequency noise is being detected in the absence of useful signal. Using state-of-the-art signal detection and processing techniques, a PD detection sensitivity somewhat better than this can be achieved. For example, several power frequency cycles can be digitized at something like 50 MS/s to give about a 20 MHz bandwidth, and then the PD can be extracted from the recorded data off line, using wavelet analysis, which would improve the PD detection sensitivity by roughly a factor of 6 from that shown for voltage detection at 20 MHz bandwidth, to the range of 20 pC for short distances to the range of 200 pC at 1000 m. As is discussed below, PD detection is not the only issue, as the PD must also be located with reasonable accuracy.

For the idealization of a Gaussian pulse in white noise, the PD detection sensitivity is determined solely by the noise, i.e.,

by the incoherent background electromagnetic interference. To improve the voltage PD detection sensitivity by a factor of 10, the voltage noise floor would have to be reduced by a factor of 10, to about 0.3 μV/√Hz from the 3 μV/√Hz assumed in Figure 10. The noise floor will vary with the environment with the 3 μV/√Hz employed in the present analysis is more typical of an urban or industrial environment than a rural environment. If the noise were reduced by two orders of magnitude from that assumed, to the range of 30 nV/√Hz, the fixed (20 MHz) bandwidth sensitivity would be reduced to about 1 pC at short distances and about 60 pC at 5000 m (3 miles). However the thermal noise in a 30 Ω transmission line is about 0.7 nV/√Hz, not taking into account the additional noise added by the front end amplifier in the detection chain which is almost certain to raise this to over 1 nV/√Hz , which makes a noise floor in the range of 30 nV/√Hz under field conditions unlikely. The more likely range of the noise floor is from 0.3 μV/√Hz under best case conditions to greater than the assumed.3 μV/√Hz under worst case conditions, which results in a typical range of PD detection sensitivity within the range shown in Figure 11.

4.4 FREQUENCY SELECTIVE PD DETECTION

An examination of Figure 9 indicates limited spectral regions with very low noise, such as between 110 and 130 MHz (just above the FM radio band) and near 30 MHz and 50 MHz. The noise is about 0.3 μV/√Hz around 120 MHz and 0.5 μV/√Hz at 30 and 50 MHz. These noise levels are about an order of magnitude lower than the "general" background level seen in Figure 9. If the PD detection is bandwidth limited to such a region, then the background noise level is very low, although the bandwidth is also limited. Detection in the 100 MHz region is only useful for PD sources near to the coupler (in the range of 20 to 50 m), while the useful range at 30 MHz would be hundreds of meters. Under some conditions, low noise spectral regions will occur at lower frequencies, which facilitate sensitive detection over larger distances, although with an inevitable reduction in sensitivity caused by the restricted bandwidth. The restricted bandwidth implicit in the use of a filter will cause a reduction in the S/N ratio roughly equal to of the square root of the ratio of the filter bandwidth to the optimum detection bandwidth for a background of white noise. This penalty will reduce as the distance to the PD source increases, i.e., as the optimum detection bandwidth decreases (Figure 9). Thus the "filter bandwidth penalty" will be greatest for nearby PD sources, but such sources are usually easy to detect. If the alternative to the restricted bandwidth of the filter is much more noise outside the bandwidth of the filter, the restricted bandwidth can be an advantage.

4.5 EFFECT OF AVERAGING

As is well known, signals are usually coherent and noise is usually random (incoherent). Thus if multiple signals can be averaged, the S/N can be improved, as the signals add coherently (proportional to the number averaged) while the noise adds incoherently (as the square root of number averaged). Averaging of PD is problematic as a result of its somewhat random character; however, "averaging" can be carried out in many contexts, such as autocorrelation, or through use of a swept frequency spectrum analyzer where several PD pulses can be expected as the filter sweeps across a resolution element. As noted above, the problem with triggering on a PD signal above the noise is that the effective peak noise is roughly 4 times the RMS value, which reduces sensitivity and makes signals below the noise undetectable by simple triggering. As well, the error in determining the time of arrival, discussed below, will reduce the effectiveness of the averaging. The oldest but perhaps most effective form of averaging in this context may be through use of a swept filter spectrum analyzer, for which the number of PD pulses within the "sampling time" of the swept filter will be averaged. Thus if the time required for the filter to sweep through the filter resolution is 1 s, then 1 s worth of PD pulses will be averaged at the frequency of the filter. This could give an improvement in S/N in the range of 10 to 30 and improve the PD detection sensitivity into the pC or sub-pC range. As is implicit in eqn. (9) as well as Figure 8, the useful bandwidth of the PD pulse reduces as a function of distance propagated. Thus in the frequency domain, the signal must be examined at a number of frequencies in order to assure that a PD pulse over the full range of detectable distances will be detected. In the time domain, this corresponds to looking for PD pulses over a wide range of pulse width, as indicated by Figure 2.

4.6 PD LOCATION

In many cases, PD location is nearly as important as detection. The subject of PD location has been examined exhaustively by Steiner, Reynolds and Weeks [6]. A reasonably good S/N ratio is required for accurate PD location. For a Gaussian pulse in white noise, the standard deviation of the measured pulse arrival time is given by

$$\Delta = \frac{\sigma\sqrt{2}}{\sqrt{\eta}} \tag{19}$$

where, as usual, σ characterizes the pulse width, and η is the signal to noise ratio [7]. After propagating 1000 m, σ is in the range of 90 ns (pulse width of ~220 ns) according to equation (10) or nearly 200 times greater than the initial PD pulse. According to equation (19), the standard deviation in the time of arrival will be about 70 ns for a S/N ratio of 10 dB (3.16), which corresponds to a propagation distance of about 10 m (35 ft). To achieve reasonable location accuracy, a S/N in the range of 40 dB (100) is required which would result in a standard deviation of 13 ns. Thus as the pulse spreads, the PD detection S/N must increase in order to maintain reasonable PD location accuracy, which decreases the detection sensitivity insofar as PD location is required.

5 CONCLUSIONS

Analytic equations have been developed which characterize propagation of a Gaussian pulse on a cable with an attenuation constant which is proportional to frequency, as is common for shielded power cables. This formulation has been extended to asymmetric PD waveforms through superposition of Gaussians in a manner which can be applied to any waveform which can be expressed as a sum of Gaussians, almost any waveform. As seen in Figure 7, the Gaussian and asymmetric waveforms result in substantially differing PD amplitudes for distance less than about 300 m, beyond which the amplitude of the two pulse waveforms merge, which implies that the optimum detection bandwidth of the two pulse waveforms also differ at short distances.

ACKNOWLEDGMENTS

Dr. John Densley encouraged the authors to pursue an analytical solution for the asymmetric PD pulse, and without his "push," the authors would probably have avoided this difficult problem. Prof. Eberhard Lemke provided encouragement, numerous helpful comments, and, after the paper was submitted, some experimental confirmation of the theory. The field noise data provided by Dr. Liming Zhou of DTE Cablewise are appreciated greatly. Figure 10 is based, in part, on discussions at the IEEE ICC with numerous experts in the area of field PD testing whose candor is appreciated.

REFERENCES

[1] Boggs, S.A. and G.C Stone, "Fundamental Limits to the Measurement of Corona and Partial Discharge", IEEE Trans Electr. Insul., Vol.17, pp. 143-150, 1982.

[2] N. Oussalah, Y. Zebboudj and S.A. Boggs, "PD Pulse Propagation in Shielded Power Cable for Symmetric and Asymmetric PD pulses", IEEE Intern. Symposium Electr. Insul. (ISEI), pp. 30-33, 2006.

[3] G.C. Stone and S.A. Boggs, "Theoretical Model for the Propagation of High Frequency Signals in Shielded Power Cables", IEEE Conf. Electr. Insul. Dielectr Phenomena (CEIDP), Washington, DC, USA, pp. 275-280, 1982.

[4] E. Lemke, "Practical Experiences in On-Site PD Diagnostics Of Power Cable Accessories in Service Using the Ultra-Wide-Band (UWB) Method", Presentation to the Fall 2005 IEEE Insulated Conductors Committee. Used with permission of the author.

[5] J. Veen and P.C.J.M. van der Wiellen, "The Application of Matched filters to PD Detection and Localization", IEEE Electr. Insul. Mag., Vol. 19, No. 5, pp. 20-26, 2003.

[6] J.P. Steiner, P.H. Reynolds, and W.L. Weeks, "Estimating the Location of Partial Discharges in Cables", IEEE Trans. Electr. Insul., Vol. 27, pp. 44-59, 1992.

[7] L.A. Wainstein and V.D. Zubakov, *Extraction of Signals from Noise*, Prentice-Hall, Inc., 1962, reprinted by Dover.

Naima Oussalah received her university applied studies Diploma in 1997, the Ing. Dipl in 2000 and the Master degree in 2002 from the University A. Mira of Bejaia, Algeria. She is currently preparing her Ph.D. thesis on partial discharges in cables. Her areas of work include corona simulation using the finite element method.

Youcef Zebboudj is Professor at the University of A. Mira of Bejaia, Algeria. He received his Ph.D. degree from the University of Paris in 1988. He is the director of Labotratoire de Génie Electrique of the University of A.Mira of Bejaia. He is the author of many publications on corona discharge. He is one of the pioneers who established the generalized Peek's law.

Steven Boggs (F'92) was graduated with a B.A. from Reed College in 1968 and received his Ph.D. and MBA degrees from the University of Toronto in 1972 and 1987, respectively. He spent 12 years with the Research Division of Ontario Hydro. He was elected an IEEE Fellow for his contributions to understanding of SF_6-insulated systems. From 1987 to 1993, he was Director of Research and Engineering at Underground Systems, Inc. He is presently Director of the Electrical Insulation Research Center and Research Professor of Materials Science, Electrical Engineering, and Physics at the University of Connecticut as well as an Adjunct Professor of Electrical and Computer Engineering at the University of Toronto.